Journal of Chromatography, 599 (1992) 87–104
Elsevier Science Publishers B.V., Amsterdam

CHROMSYMP. 2545

Theory of perfusion chromatography

A. I. Liapis* and M. A. McCoy

Department of Chemical Engineering and Biochemical Processing Institute, University of Missouri–Rolla, Rolla, MO 65401-0249 (USA)

ABSTRACT

A mathematical model of perfusion chromatography was constructed for column systems. This model could describe the dynamic behavior of single- and multi-component adsorption in columns having perfusive adsorbent particles (the perfusive particles have a non-zero intraparticle fluid velocity). The model expressions for the adsorbent particles include the intraparticle mass transfer mechanisms of convection (intraparticle fluid flow) and diffusion and the mass transfer step involving the interaction between the adsorbate molecules and the active sites on the surface of the porous adsorbent particles. The continuity expression for the fluid flowing stream in the column includes the mechanism of axial dispersion. When the intraparticle fluid velocity is taken to be equal to zero in the model of perfusion chromatography, the resulting expressions could describe single- and multi-component adsorption in columns having purely diffusive particles. The perfusion chromatographic model was solved and used to study the dynamic behavior of column systems for different particle sizes, column lengths, column fluid superficial velocities, intraparticle fluid velocities and different values of the effective pore diffusivity and of the total number of active sites per volume of adsorbent. Columns with perfusive adsorbent particles and columns with purely diffusive adsorbent particles were considered in this work. The dynamics of the interaction mechanisms of the adsorption step of the systems studied in this work are (a) relatively not fast, (b) relatively fast and (c) infinitely fast. The values of certain variables which could be used to evaluate column performance, and also the breakthrough curves obtained from columns having perfusive adsorbent particles, were compared with those obtained from columns involving purely diffusive adsorbent particles. The results from the systems studied in this work suggest that for adsorption systems having relatively fast or infinitely fast interaction kinetics (that is, the dynamics of the interaction step between the adsorbate molecules and the active sites are relatively fast or infinitely fast), the use of perfusive particles could have the potential to provide improved column performance.

INTRODUCTION

The term "perfusion chromatography" was used by Afeyan *et al.* [1] for the technique that involves the flow of liquid through a porous chromatographic particle. Their perfusive particles [1] have a network of large pores (6000–8000 Å) which transect the particles (these pores are called throughpores), and also a network of smaller (500–1500 Å) interconnecting pores between the throughpores. Also, Afeyan *et al.* [1] indicated that scanning electron micrographs show that the pore network is continuous and that no point in the porous matrix is more than 5000–10 000 Å from a throughpore. The experimental data of Afeyan *et al.* [1] suggest that their perfusive particles appear to have a bidisperse [2] porous network. However, Afeyan *et al.* [1] provided no information about the pore-size distribution functions [2,3] of the network of the throughpores and of the network of the smaller interconnecting pores; also, they provided no information about the network pore connectivity [2,3].

Theoretical models have been constructed and used to describe, with reasonable accuracy, the behavior of various single- and multi-component adsorption systems involving purely diffusive porous adsorbent particles [2–16]. The theoretical models have provided significant information about (a) the behavior and the relative importance of the transport mechanisms occurring in the adsorption systems that employ purely diffusive adsorbent particles, (b) the conditions at which percolation

0021-9673/92/$05.00

threshold phenomena may occur in purely diffusive adsorbent particles and (c) the effects that the pore-size distribution, the network pore connectivity and the sizes of the adsorbate molecules and of the active sites on the surface of the adsorbent particles have on the permeability of the adsorbate molecules. Further, the theoretical models have been used to design various small- and large-scale adsorption systems. The intraparticle mass transfer mechanisms that have been considered in the models involving purely diffusive adsorbent particles [2–16] are pore diffusion, surface diffusion and the interaction step(s) between the adsorbate(s) and the active sites on the surface of the adsorbent particles. Different systems involving fast (including infinitely fast) and slow dynamics for the interaction step(s) have been considered [2–16].

In this work, a mathematical model of perfusion chromatography is constructed. The model is then used to study the dynamic behavior of adsorption columns involving perfusive adsorbent particles. It is hoped that the theoretical model of perfusion chromatography, in the first stage of its evolution, will provide useful information about the effects and the relative importance of the different transport mechanisms on the dynamic behavior of adsorption systems employing perfusive adsorbent particles. Further, the models could provide a useful basis for comparing the performance, for a given adsorption system, of perfusive adsorbent particles relative to the performance that could be obtained from purely diffusive porous adsorbent particles.

THEORY

Adsorption is considered to take place from a flowing liquid stream in a fixed bed of perfusive adsorbent particles under isothermal conditions, and the concentration gradients in the radial direction of the bed are considered to be not significant [12,15,17]. The feed solution to the bed is considered to contain n components, and m ($m < n$) solutes may compete for the available active sites for specific adsorption; also, $m + 1 \leqslant i \leqslant l (l < n)$ solutes may be non-specifically adsorbed, and $l + 1 \leqslant i \leqslant n$ solutes are simply transported by intraparticle convection and diffusion into the pores of the particles without interacting with the adsorbent [10,12]. A differential mass balance for each component in the flowing fluid stream gives

$$\frac{\partial C_{di}}{\partial t} - D_{Li}\frac{\partial^2 C_{di}}{\partial x^2} + \frac{V_f}{\varepsilon}\cdot\frac{\partial C_{di}}{\partial x} = -\frac{(1-\varepsilon)}{\varepsilon}\cdot\frac{\partial \bar{C}_{psi}}{\partial t}, \quad i = 1,2,\ldots,n \qquad (1)$$

In eqn. 1, the velocity of the fluid stream, V_f, is taken to be independent of the space variable x, because the liquid solutions encountered in many chromatographic systems are most often very dilute and the main component of the solution is the carrier fluid. For non-dilute solutions a material balance, as shown by Harwell *et al.* [18], would provide the expression for $\partial V_f/\partial x$. The pressure drop through the fixed bed, which is important in the design of an adsorption packed bed (fixed bed) system, can be determined by the methods reported by Geankoplis [19]. The initial and boundary conditions of eqn. 1 are as follows:

$$C_{di} = 0 \text{ at } t = 0,\ 0 \leqslant x \leqslant L, \qquad i = 1,2,\ldots,n \qquad (2)$$

$$\frac{V_f}{\varepsilon}\cdot C_{di} - D_{Li}\cdot\frac{\partial C_{di}}{\partial x} = \frac{V_f}{\varepsilon}\cdot C_{di,in} \text{ at } x = 0,\ t > 0, \quad i = 1,2,\ldots,n \qquad (3)$$

$$\frac{\partial C_{di}}{\partial x} = 0 \text{ at } x = L,\ t > 0, \qquad i = 1,2,\ldots,n \qquad (4)$$

The value of $C_{di,in}$ may be constant or it may vary with time. An expression for calculating D_{Li} was presented by Arnold *et al.* [20], but in certain systems the axial dispersion is so low that by setting its value equal to zero the error introduced in the prediction of the behavior of an affinity adsorption system is not significant [17,20]. When the axial dispersion coefficient is set equal to zero, eqn. 3 (with $D_{Li} = 0$) becomes

$$C_{di} = C_{di,in} \text{ at } x = 0,\ t > 0, \qquad i = 1,2,\ldots,n \qquad (5)$$

The transport of the species in the perfusive adsorbent particles is considered to involve the following mass transfer mechanisms: (a) intraparticle convection (flow of liquid through the porous perfusive adsorbent particle), (b) diffusion in the pore fluid (pore diffusion), (c) diffusion on the pore surfaces (surface diffusion) and (d) the mass transfer step involving the interaction of the adsorbates with the active sites on the surface of the pores [this step represents the adsorption mechanism; species adsorbed by specific interaction(s), in addition to non-specifically adsorbed components, may be con-

sidered]. The adsorption process is considered to be isothermal as the heats of adsorption apparently do not change the temperature [1,3–10,12,13,15–17,20–23] of the liquid phase even in large-scale systems; this occurs because the total amount of adsorbed material is small and the heat capacity of the liquid phase is high. The differential mass balance for each component i in a perfusive adsorbent particle of slab geometry is given by

$$\varepsilon_p \cdot \frac{\partial C_{pi}}{\partial t} + \varepsilon_p v_p \cdot \frac{\partial C_{pi}}{\partial z} + \frac{\partial C_{si}}{\partial t} = \sum_{j=1}^{n} \frac{\partial}{\partial z}\left(\varepsilon_p D_{pij} \frac{\partial C_{pj}}{\partial z}\right) + \sum_{j=1}^{n} \frac{\partial}{\partial z}\left(D_{sij} \frac{\partial C_{sj}}{\partial z}\right), \qquad i = 1, 2, \ldots, n \tag{6}$$

In eqn. 6, the terms $\partial C_{si}/\partial t$ and $\partial C_{sj}/\partial z$ become equal to zero for species which do not bind by specific or non-specific adsorption. Further, if the particle porosity, ε_p, changes in a significant quantitative way because of the adsorbate(s) loading on the surface of the pores [3], then the first two terms in the left-hand side of eqn. 6 should be replaced by $\partial(\varepsilon_p C_{pi})/\partial t$ and $v_p[\partial(\varepsilon_p C_{pi})/\partial z]$, respectively. Also, if v_p changes in a significant quantitative way, because the adsorbate(s) loading on the surface of the pores may be changing the particle permeability [3], then the term $\varepsilon_p v_p(\partial C_{pi}/\partial z)$ in eqn. 6 should be replaced by $\partial(\varepsilon_p v_p C_{pi})/\partial z$. It is worth mentioning at this point that v_p may also change if the solution is non-dilute and significant amounts of adsorbate(s) are adsorbed within the particle; it is considered that this latter kind of v_p change would not occur often because in most systems the solutions are dilute and the size of the particle is small. It should also be noted that if the loading of the particles changes in a significant way the size of the radii of the pores, and because of that the pore-size distribution and pore connectivity changes, then the values of the diffusion coefficients (like the values of D_{pij}) could be changing with the local loading on the pore surfaces [3], and the phenomenon of percolation threshold [3] could appear to be possible in one or more of the porous networks located between the throughpores of the perfusive particles.

The mixtures of components to be separated by chromatographic systems are usually dilute (this is most often the case for mixtures of biological macromolecules), especially with respect to the component(s) of interest, and therefore it may be possible to set the off-diagonal ($D_{pij}, i \neq j$; $D_{sij}, i \neq j$) elements of the effective pore diffusivity matrix, $\mathbf{D}_p$, and of the surface diffusivity matrix, $\mathbf{D}_s$, equal to zero [13,15,24,25]. In this case, eqn. 6 would take the following form

$$\varepsilon_p \cdot \frac{\partial C_{pi}}{\partial t} + \varepsilon_p v_p \cdot \frac{\partial C_{pi}}{\partial z} + \frac{\partial C_{si}}{\partial t} = \frac{\partial}{\partial z}\left[\varepsilon_p D_{pi} \cdot \frac{\partial C_{pi}}{\partial z} + D_{si} \cdot \frac{\partial C_{si}}{\partial z}\right], \qquad i = 1, 2, \ldots, n \tag{7}$$

In eqn. 7, D_{pi} and D_{si} represent the diagonal terms ($D_{pij}, i = j$; $D_{sij}, i = j$) of the diffusivity matrices $\mathbf{D}_p$ and $\mathbf{D}_s$. If the interaction between the adsorbate(s) and the active sites on the surface of the pores is strong, then the surface diffusion may, in certain systems, be neglected. If the contribution of surface diffusion to mass transfer is insignificant, then eqn. 7 would become

$$\varepsilon_p \cdot \frac{\partial C_{pi}}{\partial t} + \varepsilon_p v_p \cdot \frac{\partial C_{pi}}{\partial z} + \frac{\partial C_{si}}{\partial t} = \frac{\partial}{\partial z}\left(\varepsilon_p D_{pi} \cdot \frac{\partial C_{pi}}{\partial z}\right), \qquad i = 1, 2, \ldots, n \tag{8}$$

It is clear that eqn. 8 cannot be solved if an appropriate expression for the term $\partial C_{si}/\partial t$ is not available. This term represents the accumulation of the adsorbed species i on the internal surface of the perfusive adsorbent particle, and it can be quantified if a thermodynamically consistent mathematical model could be constructed that could describe the mechanism of adsorption for component i. For isothermal adsorption systems, the term $\partial C_{si}/\partial t$ could be of the form

$$\frac{\partial C_{si}}{\partial t} = f_i(\mathbf{C}_p, \mathbf{C}_s, \mathbf{k}), \qquad i = 1, 2, \ldots, m, m+1, \ldots, l \tag{9}$$

where f_i represents the functional form of the dynamic adsorption mechanism for component i; $\mathbf{C}_p$ represents the concentration vector of the adsorbates in the pore fluid, $\mathbf{C}_p = (C_{p1}, C_{p2}, \ldots, C_{pm}, C_{pm+1}, \ldots, C_{pl})$; $\mathbf{C}_s$ denotes the concentration vector of the adsorbates in the adsorbed phase, $\mathbf{C}_s = (C_{s1}, C_{s2}, \ldots, C_{sm}, C_{sm+1}, \ldots, C_{sl})$; and $\mathbf{k}$ represents the

vector of the rate constants that characterize the interaction kinetics between the adsorbates and the active sites. For certain single- and multi-component adsorption systems, dynamic adsorption models of the form given in eqn. 9 have been constructed and presented in the literature [9,10,15,16,21,23,26,27].

In some adsorption systems, the rates of interaction between the adsorbates and the active sites may be much higher than the intraparticle convection and diffusional rates, and in such systems it may be possible to assume that equilibrium exists between the adsorbates in the pore fluid and in the adsorbed phase at each point in the pores. In this case, one would need to have thermodynamically consistent mathematical expressions that could describe the equilibrium adsorption isotherms of the adsorbates. Various mathematical expressions (developed from equilibrium adsorption models) for single- and multi-component equilibrium adsorption isotherms have been presented in the literature [4,6,8–11,14,21,22,26–32]. The term $\partial C_{si}/\partial t$ in eqn. 8, for systems where adsorption equilibrium may be assumed between the adsorbates in the pore fluid and in the adsorbed phase at each point in the pores, is then given by

$$\frac{\partial C_{si}}{\partial t} = \sum_{j=1}^{l}\left(\frac{\partial g_i}{\partial C_{pj}}\right)\left(\frac{\partial C_{pj}}{\partial t}\right), \qquad i = 1,2,\ldots,m, \; m+1,\ldots,l \tag{10}$$

where

$$C_{si} = g_i(\mathbf{C}_p, \mathbf{K}), \qquad i = 1,2,\ldots,m,m+1,\ldots,l \tag{11}$$

The functions g_i represent the equilibrium adsorption isotherms for the adsorbates that may compete for the available (accessible) active sites on the surface of the pores. **K** represents the vector of the equilibrium constants that characterize the equilibrium interactions between the adsorbates and the active sites.

The initial and boundary conditions for eqn. 8 and the initial condition for eqn. 9 are as follows:

at $t = 0$ $C_{pi} = 0$ for $0 \leqslant z \leqslant z_0$, $\quad i = 1,2,\ldots,n$ (12)

at $z = 0$ $C_{pi} = C_{di}$, $t > 0$, $\quad i = 1,2,\ldots,n$ (13)

at $z = z_0$ $C_{pi} = C_{di}$, $t > 0$, $\quad i = 1,2,\ldots,n$ (14)

at $t = 0$ $C_{si} = 0$ for $0 \leqslant z \leqslant z_0$, $\quad i = 1,2,\ldots,m,m+1,\ldots,l$ (15)

Eqns. 13 and 14 were obtained from the assumption that the external mass transfer resistance (the mass transfer resistance in a liquid film that may be located on the external particle surface) is not significant. Detailed calculations [12,16,33,34] for adsorption columns involving purely diffusive particles have shown that the intraparticle mass transfer resistance of a purely diffusive particle is significantly larger than the external mass transfer resistance, for the bulk flow-rates that are usually encountered in adsorption columns, and hence if the external mass transfer resistance is neglected the effect on the breakthrough curve is not significant. Further, in the perfusive particles there is flow in and out of the particles, and hence one may consider that the effect of the external mass transfer resistance will be even less significant than that encountered in purely diffusive particles.

The variable $\bar{C}_{psi}$ in eqn. 1 represents the average concentration of adsorbate in the adsorbent particle and its value is obtained from the equation

$$\bar{C}_{psi} = \frac{1}{V_{pv}}\left[\int_0^{V_{pv}} C_{si}\mathrm{d}V + \int_0^{V_{pv}} \varepsilon_p C_{pi}\mathrm{d}V\right], \quad i = 1,2,\ldots,n \tag{16}$$

where V_{pv} denotes the volume of the adsorbent particle. For particles of slab geometry, eqn. 16 gives

$$\bar{C}_{psi} = \frac{1}{z_0}\left[\int_0^{z_0} C_{si}\mathrm{d}z + \int_0^{z_0} \varepsilon_p C_{pi}\mathrm{d}z\right], \quad i = 1,2,\ldots,n \tag{17}$$

For particles of spherical geometry with radius r_0, eqn. 16 provides the following expression for $\bar{C}_{psi}$ in spherical adsorbent particles:

$$\bar{C}_{psi} = \frac{3}{r_0^3}\left[\int_0^{r_0} r^2 C_{si}\mathrm{d}r + \int_0^{r_0} r^2 \varepsilon_p C_{pi}\mathrm{d}r\right], \quad i = 1,2,\ldots,n \tag{18}$$

In eqn. 18, the variable r represents the radial direction of the coordinate system for the spherical particles. The term $\partial \bar{C}_{psi}/\partial t$ in eqn. 1 is obtained by differentiating the terms of eqn. 16 with respect to time, and this operation gives

$$\frac{\partial \bar{C}_{psi}}{\partial t} = \frac{1}{V_{pv}}\left[\frac{\partial}{\partial t}\left(\int_0^{V_{pv}} C_{si}\mathrm{d}V\right) + \frac{\partial}{\partial t}\left(\int_0^{V_{pv}} \varepsilon_p C_{pi}\mathrm{d}V\right)\right], \quad i = 1,2,\ldots,n \qquad (19)$$

In order to solve eqn. 8, an expression for the intraparticle velocity v_p is needed. An equation for v_p can be constructed by considering that the driving force for convective flow across a particle is the column pressure gradient, $\Delta P/L$, which imposes a pressure Δp across a particle of length z_0, and thus one could consider that $\Delta P/L = \Delta p/z_0$; however, $\Delta p/z_0 = \mu v_p/K_p$, and $\Delta P/L$ could be obtained from an Ergun-type [35] equation. This approach would give an expression for v_p of the form

$$v_p = K_p(\alpha_1 V_f + \alpha_2 V_f^2) \qquad (20)$$

where K_p is the permeability of the porous adsorbent particle, V_f is the superficial velocity (see eqn. 1) and α_1 and α_2 are constants calculated [34] from the system properties (fluid density, fluid viscosity, bed porosity, particle size).

The dynamic behavior of the column involving perfusive adsorbent particles of slab geometry is obtained by solving simultaneously eqns. 1–4, 8, 9 and 12–15. If the axial dispersion coefficient, D_{Li}, is taken to be zero, then eqn. 5 should be used instead of eqn. 3. Further, if the adsorption step between the adsorbates and the active sites may be considered to occur infinitely fast, then the term $\partial C_{si}/\partial t$ in eqn. 8 should be replaced by the expression in the right-hand side of eqn. 10, and for this case eqns. 9 and 15 are not needed. The solution of the equations of the mathematical model of perfusion chromatography was obtained [34] by employing the numerical method of orthogonal collocation [10,12,16,33,34, 36,37] on the space variables, and the resulting ordinary non-linear differential equations were integrated [34] by using Gear's method [37], which is employed in the LSODES component of the ODEPACK [38] software package.

It should be mentioned that if the intraparticle velocity v_p is set equal to zero in eqn. 8, then the solution of the above-mentioned equations would provide the dynamic behavior of a column having purely diffusive adsorbent particles of slab geometry. If the perfusive adsorbent particles have spherical geometry, then the differential mass balance for each component i in a perfusive adsorbent particle of spherical geometry (a material balance like eqn. 8 but for spherical particles) would be given by

$$\varepsilon_p \cdot \frac{\partial C_{pi}}{\partial t} + \varepsilon_p v_{pr} \cdot \frac{\partial C_{pi}}{\partial r} + \varepsilon_p v_{p\theta} \cdot \frac{1}{r} \cdot \frac{\partial C_{pi}}{\partial \theta} + \frac{\partial C_{si}}{\partial t} = \varepsilon_p D_{pi}\left[\frac{1}{r^2} \cdot \frac{\partial}{\partial r}\left(r^2 \cdot \frac{\partial C_{pi}}{\partial r}\right) + \frac{1}{r^2 \sin\theta} \cdot \frac{\partial}{\partial \theta}\left(\sin\theta \cdot \frac{\partial C_{pi}}{\partial \theta}\right)\right], \quad i = 1,2,\ldots,n \qquad (21)$$

where v_{pr} and $v_{p\theta}$ represent the intraparticle velocity components in the r and θ directions, respectively. If ε_p and D_{pi} vary with the local loading [3] (the intraparticle velocity may also vary because of the local loading), then the variation of ε_p and D_{pi} has to be considered in eqn. 21. The velocity components v_{pr} and $v_{p\theta}$ could be obtained by solving the continuity and Navier–Stokes equations of the flowing fluid stream in the column together with the continuity and Darcy's equations of the flow in the porous particles. Appropriate initial and boundary conditions for eqn. 21 can be developed; then eqn. 21 could be solved simultaneously with the equations for C_{di} and C_{si} discussed above, in order to predict the dynamic behavior of column systems involving perfusive adsorbent particles of spherical geometry.

RESULTS AND DISCUSSION

In this work, frontal analysis results are presented for systems involving single-component adsorption. The theory of perfusion chromatography that was presented in the previous section could be used, as discussed earlier, to describe the dynamic behavior of multi-component adsorption systems when the values of the parameters in the equations of the multi-component model of perfusion chromatography could be estimated from experimental measurements and/or from appropriate constitutive equations and correlations [2–16,19–23,26–33]. In the work of Afeyan *et al.* [1], experimental data for certain multi-component systems involving perfusive adsorbent particles were presented, but the values of the parameters that characterize the rates of the mass transfer and adsorption mechanisms of those systems have not been measured. Further, the experimental data presented by Afeyan *et al.* [1] are

not sufficient for the appropriate calculation of the values of these parameters through the use of the multi-component mathematical model of perfusion chromatography presented here.

The perfusion chromatographic single-component adsorption systems examined in this work are considered to involve adsorbent particles of slab geometry and the interaction kinetics (adsorption mechanism) between the adsorbate molecules and the active sites are considered to be described by a reversible mechanism of the form

$$A + S \underset{k_2}{\overset{k_1}{\rightleftharpoons}} AS \tag{22}$$

where A represents the adsorbate molecule, S denotes the free active site on the surface, AS represents the adsorbate-active site complex and k_1 and k_2 are the rate constants that characterize the forward and reverse interaction mechanisms, respectively. If the interaction steps in expression 22 are considered to represent elementary interactions, then the dynamic equation for the mechanism in expression 22 is given by [15]

$$\frac{\partial C_s}{\partial t} = k_1 C_p (C_T - C_s) - k_2 C_s \tag{23}$$

The right-hand side of eqn. 23 represents one possible form for the function f_i in eqn. 9 for single-component adsorption; the subscript i is dropped from the equations of the perfusion chromatographic model whenever a single-component adsorption system (as is the case here) is considered. Eqn. 23 has been found to provide, for practical purposes, an adequate expression for the dynamics of the interaction between β-galactosidase and immobilized monoclonal anti-β-galactosidase [10,15, 16], and for the dynamics of the interaction between lysozyme and immobilized monoclonal anti-lysozyme [23]. In the perfusion chromatographic simulation studies in this work we examined the following single-component adsorption systems: (a) β-galactosidase interacting with immobilized monoclonal anti-β-galactosidase and (b) lysozyme interacting with immobilized monoclonal anti-lysozyme.

The monoclonal antibody molecules are considered to be immobilized on the surface of perfusive adsorbent particles of slab geometry and the dynamics of the adsorption step are described by eqn. 23. Two different values for the particle size, z_0, were considered: (i) $z_0 = 8.060 \cdot 10^{-6}$ m and (ii) $z_0 = 16.120 \cdot 10^{-6}$ m.

In Table I, the values of the parameters used in the perfusion model for the simulation of the two different single-component adsorption systems discussed above are presented; in certain simulations, the values of some of the parameters in Table I have been altered, and this is indicated in the appropriate figures by reporting the values of the parameters. Further, the values of other parameters of the perfusion model are reported in the captions of the figures. The values of the parameters in Table I are from adsorption systems reported in the literature [10,12,15,16,23] and, for the purposes of the simulations of this work, are considered to have appropriate magnitudes; it should be mentioned that the value of C_T in Table I represents the largest (maximum) amount of adsorbate that could be adsorbed per unit volume of particle.

In the simulations in this work, the dynamic behavior of the perfusion chromatographic systems was examined for the following intraparticle velocities (for a given superficial velocity, V_f): $v_p = 0$, $v_p = 0.02V_f$, $v_p = 0.03V_f$ and $v_p = 0.05V_f$. The range of the values of V_f examined in this work is similar to the experimental values considered by Afeyan *et al.* [1]. Further, the resulting range of the non-zero values of the intraparticle velocity, v_p, examined in this work is within the range suggested by the data in ref. 1 and by calculations performed

TABLE I

VALUES FOR CERTAIN PARAMETERS OF THE MODEL OF PERFUSION CHROMATOGRAPHY

System[a]	Parameters
A	$C_{d,in} = 0.1$ kg/m^3; $C_T = 2.2$ kg/m^3; $D_L = 0$; $D_p = 6.9 \cdot 10^{-12}$ m^2/s; $k_1 = 2.35 \cdot 10^{-2}$ m^3/kg · s; $k_2 = 5.17 \cdot 10^{-6}$ s^{-1}; $K = k_1/k_2 = 4.545 \cdot 10^3$ m^3/kg; $\varepsilon = 0.35$; $\varepsilon_p = 0.50$; $T = 293$ K
B	$C_{d,in} = 0.1$ kg/m^3; $C_T = 2.2$ kg/m^3; $D_L = 0$; $D_p = 17.885 \cdot 10^{-12}$ m^2/s; $k_1 = 4.108$ m^3/kg · s; $k_2 = 0.2222$ s^{-1}; $K = k_1/k_2 = 18.488$ m^3/kg; $\varepsilon = 0.35$; $\varepsilon_p = 0.50$; $T = 282.5$ K

[a] System A, β-galactosidase and monoclonal anti-β-galactosidase; system B, lysozyme and monoclonal anti-lysozyme.

with eqn. 20. It is worth noting again that the adsorbent particles are considered to be purely diffusive when $v_p = 0$.

If the dynamics of the adsorption step are considered to be infinitely fast, then adsorption equilibrium between the adsorbate in the pore fluid and in the adsorbed phase may be considered at every point in the pores, and hence $\partial C_s/\partial t$ is taken to be zero in eqn. 23. In this case, eqn. 23 would give the following equilibrium ($\partial C_s/\partial t = 0$) adsorption expression:

$$C_s = \frac{C_T K C_p}{1 + K C_p} \tag{24}$$

Eqn. 24 represents the equilibrium Langmuir adsorption expression [4,9,10,15,16,39] and K is the equilibrium adsorption constant ($K = k_1/k_2$). The right-hand side of eqn. 24 represents one possible form for the function g_i in eqn. 11 for single-component adsorption; the subscript i is dropped from the equations of the perfusion chromatographic model whenever a single-component adsorption system (as is the case here) is considered. When eqn. 24 is employed in the right-hand side of eqn. 10, the following expression is obtained for $\partial C_s/\partial t$:

$$\frac{\partial C_s}{\partial t} = \left(\frac{\partial C_s}{\partial C_p}\right)\left(\frac{\partial C_p}{\partial t}\right) = \left[\frac{C_T K}{(1 + K C_p)^2}\right]\left(\frac{\partial C_p}{\partial t}\right) \tag{25}$$

In this work, the dynamic behavior of a perfusion chromatographic system (single-component adsorption system) with infinitely fast dynamics for the adsorption step was also examined (for purposes of comparison with a system having finite dynamics of interaction), and the expression for the term $\partial C_s/\partial t$ in eqn. 8 was represented by eqn. 25. For this adsorption system, the value of C_T was taken to be equal to 2.2 kg/m^3 (this value is the same as that used in the systems in Table I), and the value of the equilibrium adsorption constant K was taken to be equal to the value for the system involving the interaction of lysozyme with immobilized monoclonal anti-lysozyme, and thus $K = k_1/k_2 = 4.108/0.2222 = 18.488$ m^3/kg.

In Figs. 1–10, the breakthrough curves for β-galactosidase and lysozyme are presented for different column lengths, particle sizes, column fluid superficial velocities (V_f) and intraparticle velocities (v_p). The results in Figs. 1 and 2 indicate that there is no significant difference between the breakthrough

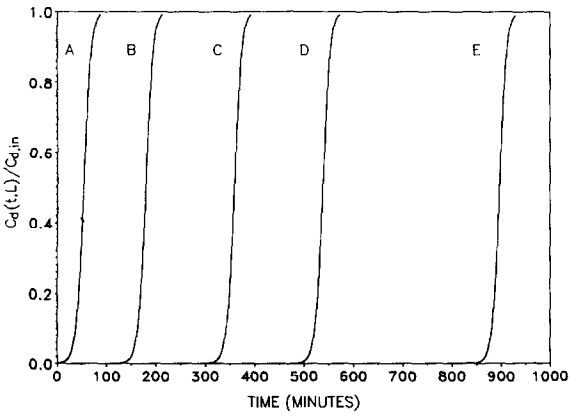

Fig. 1. Breakthrough curve of β-galactosidase: $z_0 = 8.060 \cdot 10^{-6}$ m; $V_f = 0.138 \cdot 10^{-3}$ m/s; $v_p = (0, 0.02, 0.03, 0.05)V_f$. Column lengths: (A) 0.03; (B) 0.1; (C) 0.2; (D) 0.3; (E) 0.5 m.

curves of purely diffusive ($v_p = 0$) and perfusive ($v_p > 0$) particles when $V_f = 0.138 \cdot 10^{-3}$ m/s; it can also be observed that when $z_0 = 16.120 \cdot 10^{-6}$ m, the breakthrough of β-galactosidase begins to occur slightly later for the column systems involving perfusive particles. When the superficial velocity, V_f, in the column is increased to $2.778 \cdot 10^{-3}$ m/s, then the curves in Figs. 3 and 4 clearly show that, for a given column length, the breakthrough of β-galactosidase begins to occur later for the column systems employing perfusive particles. Also, the differences

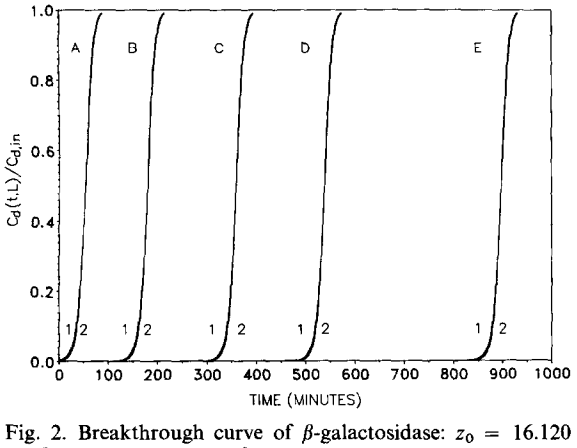

Fig. 2. Breakthrough curve of β-galactosidase: $z_0 = 16.120 \cdot 10^{-6}$ m; $V_f = 0.138 \cdot 10^{-3}$ m/s; (1) $v_p = 0$; (2) $v_p = (0.02, 0.03, 0.05)V_f$. Column lengths, (A) 0.03; (B) 0.1; (C) 0.2; (D) 0.3; (E) 0.5 m.

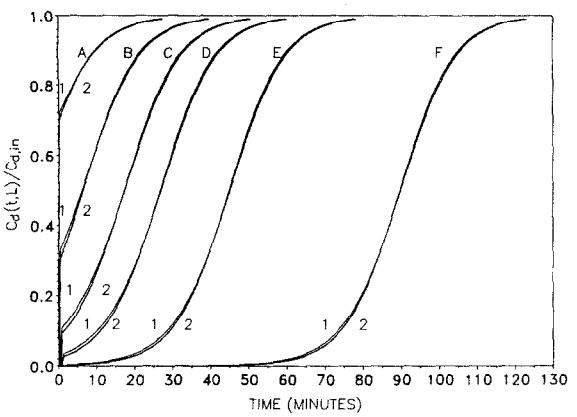

Fig. 3. Breakthrough curve of β-galactosidase: $z_0 = 8.060 \cdot 10^{-6}$ m; $V_f = 2.778 \cdot 10^{-3}$ m/s; (1) $v_p = 0$; (2) $v_p = (0.02, 0.03, 0.05)V_f$. Column lengths: (A) 0.03; (B) 0.1; (C) 0.2; (D) 0.3; (E) 0.5 m; (F) 1.0 m.

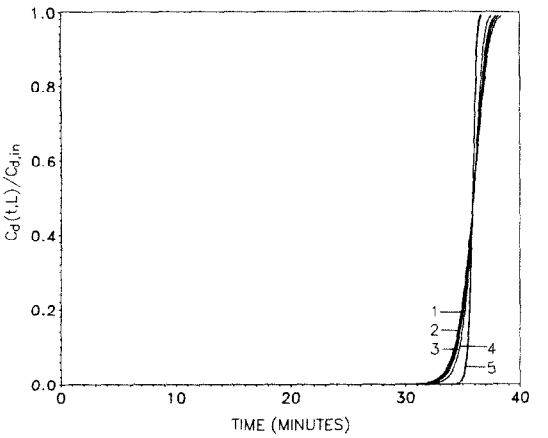

Fig. 5. Breakthrough curve of lysozyme: $V_f = 0.138 \cdot 10^{-3}$ m/s; $L = 0.03$ m; (1) $v_p = 0$, $z_0 = 16.120 \cdot 10^{-6}$ m; (2) $v_p = 0.02V_f$, $z_0 = 16.120 \cdot 10^{-6}$ m; (3) $v_p = 0.03V_f$, $z_0 = 16.120 \cdot 10^{-6}$ m; (4) $v_p = 0.05V_f$, $z_0 = 16.120 \cdot 10^{-6}$ m; (5) $v_p = (0, 0.02, 0.03, 0.05)V_f$, $z_0 = 8.060 \cdot 10^{-6}$ m.

between the β-galactosidase breakthrough curves obtained from the columns having perfusive particles and from the columns involving purely diffusive particles increase as the particle size increases. A comparison of the results in Figs. 3 and 4 indicates that, for a given column length, the breakthrough of β-galactosidase starts later when the smaller particle size is used. Further, by comparing the times at which β-galactosidase breakthrough begins (Figs. 3 and 4), it is found that the percentage difference between the initial times (initial time refers to the time at which breakthrough begins) obtained from purely diffusive and perfusive particles decreases as the column length increases. In Figs. 2–4, the relative differences in the breakthrough curves obtained from the three different non-zero v_p values are very small and could not be described graphically.

In Fig. 5, the results indicate that the differences in

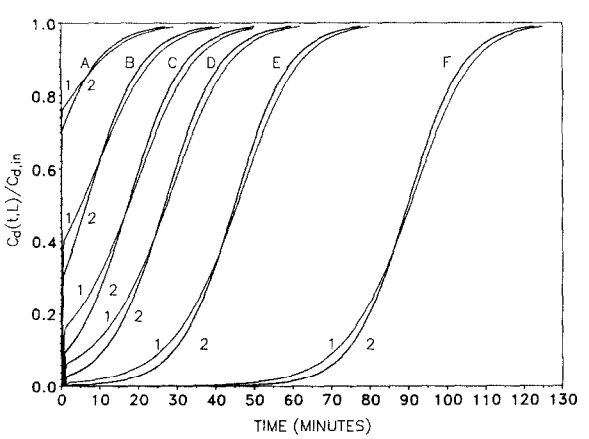

Fig. 4. Breakthrough curve of β-galactosidase: $z_0 = 16.120 \cdot 10^{-6}$ m; $V_f = 2.778 \cdot 10^{-3}$ m/s; (1) $v_p = 0$; (2) $v_p = (0.02, 0.03, 0.05)V_f$. Column lengths: (A) 0.03; (B) 0.1; (C) 0.2; (D) 0.3; (E) 0.5; (F) 1.0 m.

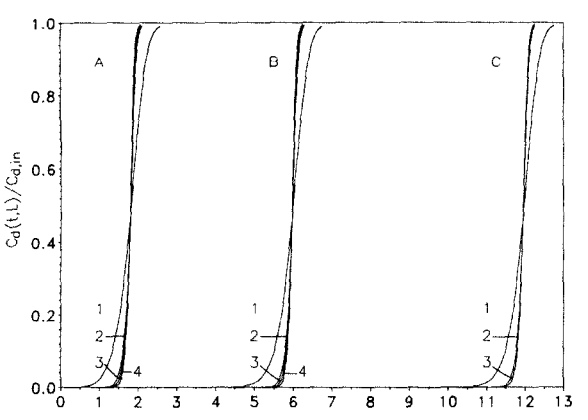

Fig. 6. Breakthrough curve of lysozyme: $V_f = 2.778 \cdot 10^{-3}$ m/s; $z_0 = 8.060 \cdot 10^{-6}$ m. Column lengths and intraparticle fluid velocities: (A) 0.03 m, (1) $v_p = 0$, (2) $v_p = 0.02V_f$, (3) $v_p = 0.03V_f$, (4) $v_p = 0.05V_f$; (B) 0.1 m, (1) $v_p = 0$, (2) $v_p = 0.02V_f$, (3) $v_p = 0.03V_f$, (4) $v_p = 0.05V_f$; (C) 0.2 m, (1) $v_p = 0$, (2) $v_p = 0.02V_f$, (3) $v_p = (0.03, 0.05)V_f$.

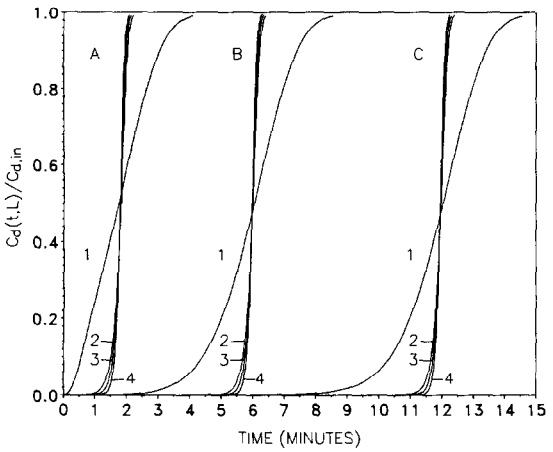

Fig. 7. Breakthrough curve of lysozyme: $V_f = 2.778 \cdot 10^{-3}$ m/s; $z_0 = 16.120 \cdot 10^{-6}$ m. Column lengths: (A) 0.03; (B) 0.1; (C) 0.2 m. For all column lengths: (1) $v_p = 0$; (2) $v_p = 0.02V_f$; (3) $v_p = 0.03V_f$; (4) $v_p = 0.05V_f$.

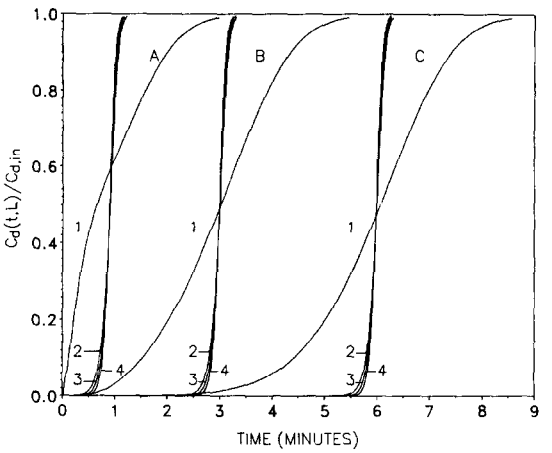

Fig. 9. Breakthrough curve of lysozyme: $V_f = 5.556 \cdot 10^{-3}$ m/s; $z_0 = 16.120 \cdot 10^{-6}$ m. Column lengths: (A) 0.03; (B) 0.1; (C) 0.2 m. For all column lengths: (1) $v_p = 0$; (2) $v_p = 0.02V_f$; (3) $v_p = 0.03V_f$; (4) $v_p = 0.05V_f$.

the lysozyme breakthrough curves obtained from purely diffusive and perfusive particles are insignificant when $z_0 = 8.060 \cdot 10^{-6}$ m and $V_f = 0.138 \cdot 10^{-3}$ m/s. For the larger particles, the data in Fig. 5 imply that the differences in the breakthrough curves are small, and the breakthrough of lysozyme begins at larger times when perfusive particles are used in the column; further, it can be observed that as the intraparticle velocity, v_p, is increased the time at which breakthrough begins is increased. Also, the data in Fig. 5 imply that the utilization of immobilized monoclonal anti-lysozyme (ligand) is higher (higher column performance) when the smaller in size particles are used.

In Figs. 6 and 7, the lysozyme breakthrough curves are shown for different column lengths and particle sizes when $V_f = 2.778 \cdot 10^{-3}$ m/s. It can be observed that the breakthrough curves obtained

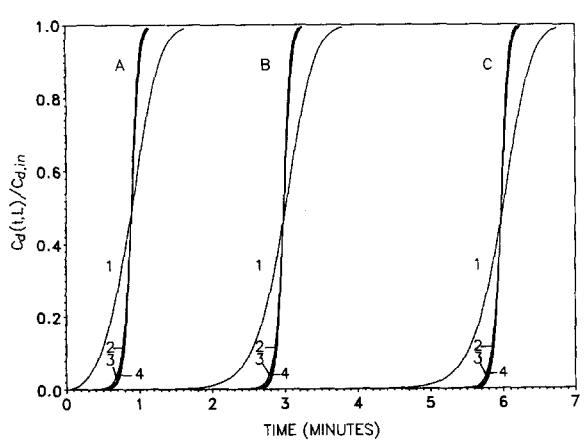

Fig. 8. Breakthrough curve of lysozyme: $V_f = 5.556 \cdot 10^{-3}$ m/s; $z_0 = 8.060 \cdot 10^{-6}$ m. Column lengths: (A) 0.03; (B) 0.1; (C) 0.2 m. For all column lengths: (1) $v_p = 0$; (2) $v_p = 0.02V_f$; (3) $v_p = 0.03V_f$; (4) $v_p = 0.05V_f$.

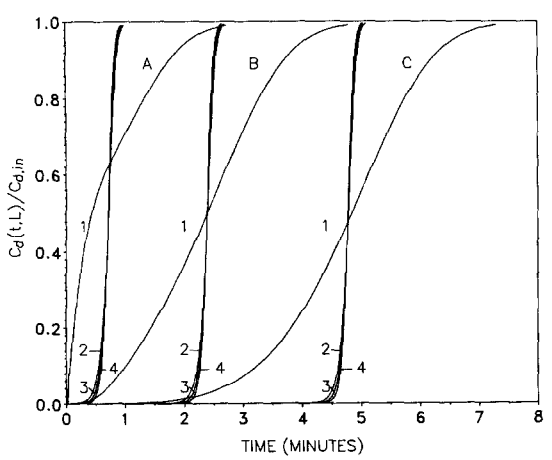

Fig. 10. Breakthrough curve of lysozyme: $V_f = 6.944 \cdot 10^{-3}$ m/s; $z_0 = 16.120 \cdot 10^{-6}$ m. Column lengths: (A) 0.03; (B) 0.1; (C) 0.2 m. For all column lengths: (1) $v_p = 0$; (2) $v_p = 0.02V_f$; (3) $v_p = 0.03V_f$; (4) $v_p = 0.05V_f$.

from the perfusive particles are very much steeper than those obtained from the purely diffusive particles. Further, the times at which breakthrough begins are significantly larger in the columns with perfusive particles, especially in the case where the larger particles are employed.

In Figs. 8 and 9, the lysozyme breakthrough curves are presented for different column lengths and particle sizes when $V_f = 5.556 \cdot 10^{-3}$ m/s. For the smaller particles (Fig. 8) the qualitative behavior is similar to that in Fig. 6, but for the larger particles (Fig. 9) the lysozyme breakthrough curves obtained from the purely diffusive particles are much more disperse than those in Fig. 7, and there is a significant difference in the shape of the breakthrough curves for the column length $L = 0.03$ m. It is also observed in Figs. 8 and 9 that the breakthrough curves obtained from the columns with perfusive particles are very steep; the significant increase in the column fluid superficial velocity, V_f, had no significant effect on the shape of the breakthrough curves obtained from the columns with perfusive particles. Further, the results in Figs. 8 and 9 show that the increased value of V_f affected, for a given column length, the time at which breakthrough begins (compare Figs. 6 and 8 and Figs. 7 and 9). By comparing the results for the perfusive particles in Figs. 6 and 7 and in Figs. 8 and 9, it is found that the time at which breakthrough begins, for a given column length, is larger when the smaller particles are used.

In Fig. 10, the lysozyme breakthrough curves are shown when $V_f = 6.944 \cdot 10^{-3}$ m/s and $z_0 = 16.120 \cdot 10^{-6}$ m. By comparing the results in Figs. 9 and 10, it can be observed again that the columns with perfusive particles provide very steep breakthrough curves. The data in Figs. 6–10 also show that as the intraparticle velocity, v_p, is increased (for the values of the superficial velocity considered in Figs. 6–10), the time at which breakthrough begins, for a given column length, is increased.

An analysis of the dynamic behavior of the two different adsorption systems in Table I indicated that the differences in the dynamic behavior (Figs. 1–10) of β-galactosidase and lysozyme depend significantly on (i) the differences in the values of k_1, the value of k_1 characterizing the formation of the adsorbate–ligand complex ($k_1 = 2.35 \cdot 10^{-2}$ for β-galactosidase and 4.108 for lysozyme), and (ii) the differences in the values of the effective pore diffusivities of β-galactosidase and lysozyme ($D_p = 6.9 \cdot 10^{-12}$ for β-galactosidase and $17.885 \cdot 10^{-12}$ for lysozyme). The ratio of the k_1 value of the lysozyme–anti-lysozyme system to that of the β-galactosidase–anti-β-galactosidase system is $1.748 \cdot 10^2$, and the ratio of the D_p value of lysozyme to that of β-galactosidase is 2.592. The analysis has indicated that, although the equilibrium adsorption constant of the β-galactosidase–anti-β-galactosidase system is significantly larger than that of the lysozyme–anti-lysozyme system (see Table I), the breakthrough curves of lysozyme obtained from the columns with perfusive particles are much steeper than the corresponding breakthrough curves of β-galactosidase, because the values of k_1 and D_p of the lysozyme–anti-lysozyme system are significantly larger than those of the β-galactosidase–anti-β-galactosidase system.

In Fig. 11, the concentration profiles of lysozyme in the pore fluid and in the adsorbed phase of a single particle of slab geometry are shown. This particle is located within the column at a position $x = 6.6645 \cdot 10^{-5}$ m from the column entrance, and the concentration profiles are shown for time $t = 0.05$ min. It can be clearly observed that for the purely diffusive

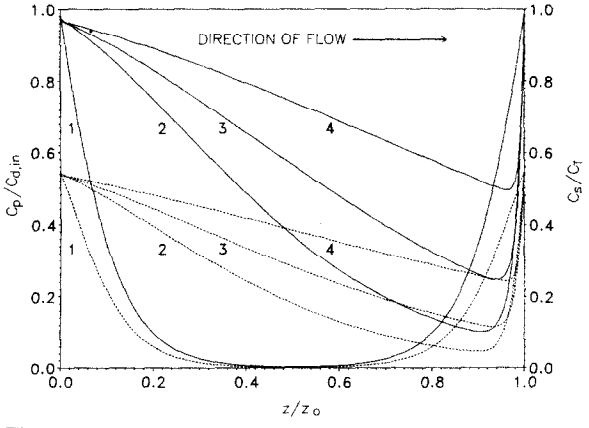

Fig. 11. Dimensionless concentration profiles of lysozyme in the pore fluid and in the adsorbed phase of the porous adsorbent particle at time $t = 0.05$ min and at position $x = 6.6645 \cdot 10^{-5}$ m in the column. $V_f = 2.778 \cdot 10^{-3}$ m/s; $z_0 = 16.120 \cdot 10^{-6}$ m; column length, $L = 0.03$ m. The data for the solid curves represent $C_p/C_{d,in}$ *versus* z/z_0. The data for the broken curves represent C_s/C_f *versus* z/z_0. For the solid and broken curves the intraparticle fluid velocities are (1) $v_p = 0$; (2) $v_p = 0.02V_f$; (3) $v_p = 0.03V_f$; (4) $v_p = 0.05V_f$.

particle ($v_p = 0$) the concentration of lysozyme in the pore fluid and in the adsorbed phase is about equal to zero in a significant portion of the particle; further, the concentration profiles of the purely diffusive particle are symmetrical, as expected, and the point of symmetry is located at the center of the particle where $z/z_0 = 0.5$. For the perfusive particle ($v_p > 0$), it is observed that the concentrations of lysozyme in the pore fluid and in the adsorbed phase are non-zero at every point in the particle, and this makes the average concentration of lysozyme in the pore fluid and in the adsorbed phase of the perfusive particle higher than that in the pore fluid and in the adsorbed phase of the purely diffusive particle. Further, the results in Fig. 11 show that as the intraparticle velocity, v_p, increases, the concentration minimum in the pore fluid and the concentration minimum in the adsorbed phase move downstream while the overall lysozyme content of the particle increases.

Certain interesting aspects of column performance could be studied by examining some characteristic pieces of information of the dynamic behavior of a given column. When the value of C_p in the equilibrium isotherm expression is equal to the inlet concentration of the adsorbate, $C_{d,in}$, in the column, then the equilibrium isotherm expression would provide the equilibrium value for the concentration of the adsorbate in the adsorbed phase, C_s, for the given value of $C_{d,in}$. Then, by knowing the total amount of the adsorbent particles in a given column, one can calculate the equilibrium amount of adsorbate that could be adsorbed in the column for the given inlet concentration $C_{d,in}$. Hence one possible measure for evaluating the performance of a given column [it should be noted that adsorption in a column is a dynamic (non-steady-state) operation], could be the ratio of the amount of adsorbate that has been adsorbed in the particles of the column after a certain time of operation to the amount of adsorbate that could be adsorbed in the particles of the column at equilibrium. This ratio is called here relative adsorptivity; the percentage of relative adsorptivity is obtained by multiplying the relative adsorptivity by 100.

It is thought that a plot of the percentage of relative adsorptivity *versus* time could provide useful information for evaluating column performance. If, for example, a high value for the percentage of relative adsorptivity may be obtained in a shorter time, then this could imply that in a given overall operational time a larger number of adsorption cycles could be realized. Another possible measure for evaluating the performance of a given column is to examine the variation in the value of the percentage of relative adsorptivity when the percentage of breakthrough varies; the percentage of breakthrough is obtained by multiplying the dimensionless ratio $C_d(t,L)/C_{d,in}$ (see Figs. 1–10) by 100. If, for instance, a high value of the percentage of relative adsorptivity may be obtained at a low value of the

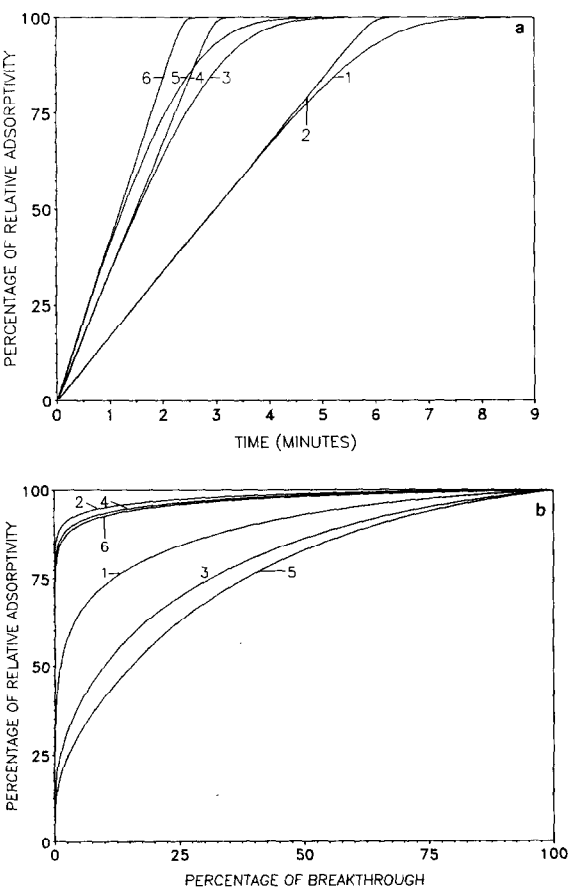

Fig. 12. Percentage of relative adsorptivity *versus* (a) time and (b) percentage of relative adsorptivity *versus* percentage of breakthrough for the lysozyme–monoclonal anti-lysozyme adsorption system. In both instances $L = 0.1$ m; $z_0 = 16.120 \cdot 10^{-6}$ m; (1) $V_f = 2.778 \cdot 10^{-3}$ m/s, $v_p = 0$; (2) $V_f = 2.778 \cdot 10^{-3}$ m/s, $v_p = 0.02V_f$; (3) $V_f = 5.556 \cdot 10^{-3}$ m/s, $v_p = 0$; (4) $V_f = 5.556 \cdot 10^{-3}$ m/s, $v_p = 0.02V_f$; (5) $V_f = 6.944 \cdot 10^{-3}$ m/s; $v_p = 0$; (6) $V_f = 6.944 \cdot 10^{-3}$ m/s, $v_p = 0.02V_f$.

percentage of breakthrough, then this could indicate that the adsorption capacity of the particles may have been utilized effectively and the total amount of adsorbate that left the column (before the introduction of column switch) may be not large.

It is thought that a plot of the percentage relative adsorptivity *versus* the percentage of breakthrough could provide useful information for evaluating column performance. In Fig. 12a the percentage of relative adsorptivity for lysozyme is plotted *versus* time and in Fig. 12b it is plotted *versus* the percentage of breakthrough, for a column length of 0.1 m and for different superficial and intraparticle velocities.

The results in Fig. 12a indicate that, for a given time, the highest value of the percentage of relative adsorptivity is obtained when perfusive particles are employed and the superficial velocity has its highest value. Also, for a given time and a given superficial velocity, the perfusive particles provide a higher value of the percentage of relative adsorptivity; further, the differences in the values of the percentage of relative adsorptivity obtained from the purely diffusive and perfusive particles increase when the superficial velocity increases, as well as when the time increases.

The results in Fig. 12b indicate that for a given percentage of breakthrough, the perfusive particles provide a higher value of the percentage of relative adsorptivity. It is also observed that, for a given percentage of breakthrough, the value of the percentage of relative adsorptivity increases as the superficial velocity decreases; the effect of the superficial velocity on the percentage of relative adsorptivity is significantly smaller when perfusive particles are used and practical values for the percentage of breakthrough are considered.

The information in Fig. 12a and b may also be used as follows: for a selected percentage of breakthrough, the value of the percentage of relative adsorptivity is obtained from the appropriate curve in Fig. 12b; this value is then utilized with the appropriate curve in Fig. 12a to obtain the time at which the selected percentage breakthrough will occur. From the above discussion, it is suggested that by examining the kind of information shown in Fig. 12a and b, one could develop operating conditions (after appropriate optimization) that could provide the desired column performance.

Another aspect of the perfusive particles that is examined in this work is the effect of the variation of C_T on column performance. If, for example, one could develop a purely diffusive particle whose pore-size distribution could provide an accessible active surface whose area is larger than that of the perfusive particle, when both the purely diffusive and perfusive particles have the same kind of active surface and the same particle size, then this could suggest that the value of C_T in the purely diffusive particle may be larger than the value of C_T in the perfusive particle. Further, the pore-size distribution of the perfusive particle, the lengths of the throughpores and the distances between the throughpores may result in an effective pore diffusivity for the adsorbate in the perfusive particle that has a higher value than the effective pore diffusivity of the adsorbate in the purely diffusive particle.

It was considered worth examining the effects that the variation of C_T and D_p may have on the dynamic behavior of a column system. In Figs. 13a and 14a, the percentage of relative adsorptivity is plotted *versus* time for the adsorption systems in Table I and for different values of C_T, D_p and v_p. In Figs. 13b and 14b, the percentage of relative adsorptivity is plotted *versus* the percentage of breakthrough for the same adsorption systems and values of C_T, D_p and v_p, as in Figs. 13a and 14a.

The results in Fig. 13a and b indicate that for the β-galactosidase–anti-β-galactosidase system, an increase of 10% in the value of D_p does not appear to have a significant effect on column behavior; the results in Fig. 13b indicate that an increase in the value of D_p by 10% has a small influence on the behavior of the column having purely diffusive particles whereas the effect on the column involving perfusive particles appears to be insignificant. When the value of C_T is reduced by 10%, the results in Fig. 13a and b indicate that the reduction in the C_T value may have a considerable effect on the behavior of a column having purely diffusive or perfusive particles. A comparison of the results expressed by curves 1 and 6 and by curves 3 and 8 in Fig. 13b indicates that the value of the percentage of relative adsorptivity obtained from the perfusive particles, for a given practical value of the percentage of breakthrough, is higher than that obtained from the purely diffusive particles, although the value of C_T of the purely diffusive particles is taken to be 10%

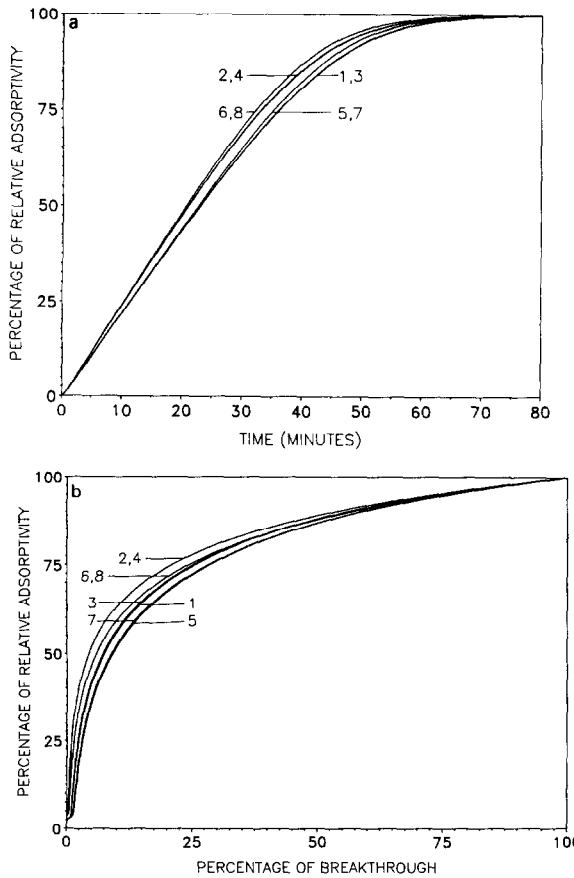

Fig. 13. Percentage of relative adsorptivity *versus* (a) time and (b) percentage of breakthrough for the β-galactosidase–monoclonal anti-β-galactosidase adsorption system. In both instances L = 0.5 m; z_0 = 16.120 · 10^{-6} m; V_f = 2.778 · 10^{-3} m/s; (1) C_T = 2.2 kg/m^3, D_p = 6.9 · 10^{-12} m^2/s, v_p = 0; (2) C_T = 2.2 kg/m^3, D_p = 6.9 · 10^{-12} m^2/s, v_p = 0.02V_f; (3) C_T = 2.2 kg/m^3, D_p = 1.1 · (6.9 · 10^{-12}) m^2/s, v_p = 0; (4) C_T = 2.2 kg/m^3, D_p = 1.1 · (6.9 · 10^{-12}) m^2/s, v_p = 0.02V_f; (5) C_T = 0.9 · (2.2) kg/m^3, D_p = 6.9 · 10^{-12} m^2/s, v_p = 0; (6) C_T = 0.9 · (2.2) kg/m^3, D_p = 6.9 · 10^{-12} m^2/s, v_p = 0.02V_f; (7) C_T = 0.9 · (2.2) kg/m^3, D_p = 1.1 · (6.9 · 10^{-12}) m^2/s, v_p = 0; (8) C_T = 0.9 · (2.2) kg/m^3, D_p = 1.1 · (6.9 · 10^{-12}) m^2/s, v_p = 0.02V_f.

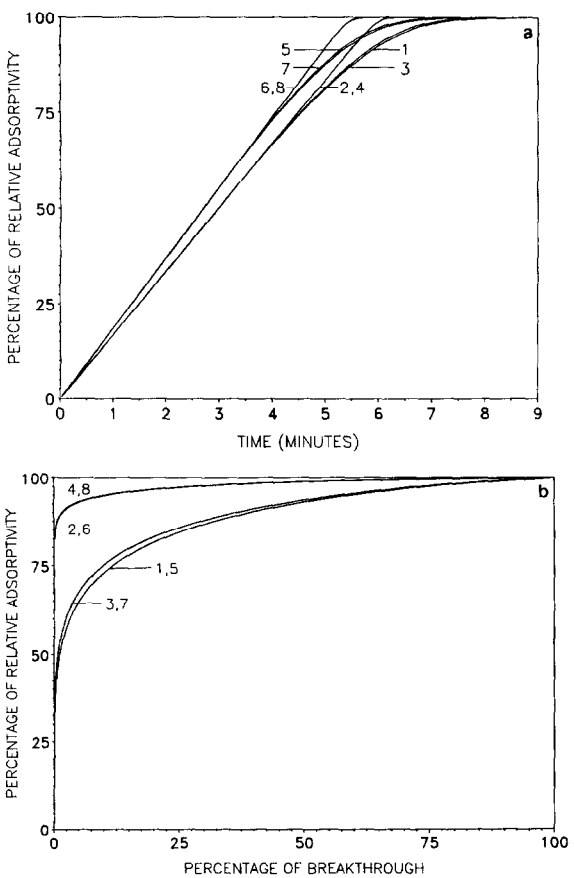

Fig. 14. Percentage of relative adsorptivity *versus* (a) time and (b) percentage of breakthrough for the lysozyme–monoclonal anti-lysozyme adsorption system. In both instances L = 0.1 m; z_0 = 16.120 · 10^{-6} m; V_f = 2.778 · 10^{-3} m/s; (1) C_T = 2.2 kg/m^3, D_p = 17.885 · 10^{-12} m^2/s, v_p = 0; (2) C_T = 2.2 kg/m^3, D_p = 17.885 · 10^{-12} m^2/s, v_p = 0.02V_f; (3) C_T = 2.2 kg/m^3, D_p = 1.1 · (17.885 · 10^{-12}) m^2/s, v_p = 0; (4) C_T = 2.2 kg/m^3, D_p = 1.1 · (17.885 · 10^{-12}) m^2/s, v_p = 0.02V_f; (5) C_T = 0.9 · (2.2) kg/m^3, D_p = 17.885 · 10^{-12} m^2/s, v_p = 0; (6) C_T = 0.9 · (2.2) kg/m^3, D_p = 17.885 · 10^{-12} m^2/s, v_p = 0.02V_f; (7) C_T = 0.9 · (2.2) kg/m^3, D_p = 1.1 · (17.885 · 10^{-12}) m^2/s, v_p = 0; (8) C_T = 0.9 · (2.2) kg/m^3, D_p = 1.1 · (17.885 · 10^{-12}) m^2/s, v_p = 0.02V_f.

larger than the C_T value of the perfusive particles.

The results in Fig. 14a indicate that for the lysozyme–anti-lysozyme system, an increase of 10% in the value of D_p does not appear to have a significant effect on column behavior; an increase in the value of D_p by 10% has a small influence on the behavior of the column having purely diffusive particles, and this appears to occur only at longer times of operation. When the value of C_T is reduced by 10%, the results in Fig. 14a indicate that the reduction in the C_T value may have a considerable effect on the dynamic behavior of a column having purely diffusive or perfusive particles. The data in Fig. 14b suggest that for practical values of the percentage of breakthrough, an increase in the value of D_p by 10% has some effect on the value of relative

adsorptivity obtained from the columns having purely diffusive particles, whereas it has an insignificant effect on the value of the percentage of relative adsorptivity obtained from the columns with perfusive particles. In Fig. 14b, it is also observed that the effect of the reduced value of C_T on the percentage of relative adsorptivity, for a given practical value of the percentage of breakthrough, is not significant for this adsorption system. A comparison of the results in Fig. 14b indicates that the value of the percentage of relative adsorptivity obtained from the perfusive particles is higher than that obtained from the purely diffusive particles, even when the value of C_T of the perfusive particles is 10% smaller than the C_T value of the purely diffusive particles.

It is worth mentioning again here that the dynamics of the interaction kinetics of the lysozyme–anti-lysozyme adsorption system are faster than those of the β-galactosidase–anti-β-galactosidase adsorption system, and that the effective pore diffusivity of lysozyme is higher than that of β-galactosidase; these differences were found to be responsible for the differences observed in the dynamic behavior of these systems. It should be noted that by combining and examining (as discussed above for Fig. 12a and b) the kind of information shown in Fig. 13a and b or in Fig. 14a and b, one could develop operating conditions (by varying, for example, the values of V_f, v_p and L, and performing appropriate system optimization) that could provide the desired column performance under conditions of variation (or uncertainty) in the values of C_T and D_p.

In Figs. 15 and 16, the breakthrough curves of lysozyme when the interaction of lysozyme with immobilized monoclonal anti-lysozyme is taken to be infinitely fast (eqn. 25), are shown for different particle sizes and intraparticle velocities. It can be observed (as was the case when the results in Figs. 6 and 7 were compared) that the effect of particle size on the breakthrough curve of lysozyme obtained from purely diffusive particles is very significant, whereas the magnitude of the effect is considerably smaller when perfusive particles are employed in the column. The breakthrough curves obtained from the perfusive particles are very steep and, for a given particle size, the time at which breakthrough begins is increased as the intraparticle velocity, v_p, increases. Further, for a given intraparticle velocity, v_p, the time at which breakthrough begins is increased as the particle size decreases.

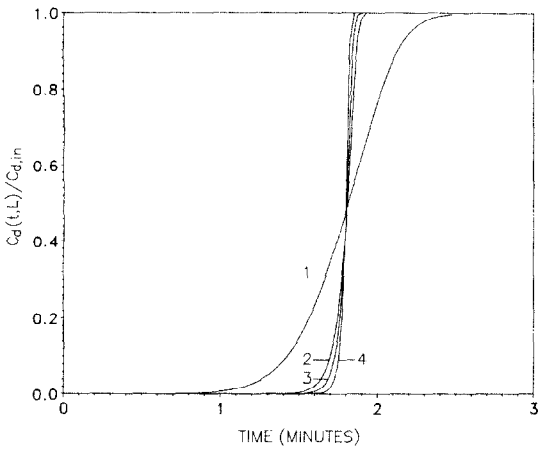

Fig. 15. Breakthrough curve of lysozyme when the dynamics of the interaction kinetics of the adsorption step are taken to be infinitely fast. $L = 0.03$ m; $z_0 = 8.060 \cdot 10^{-6}$ m; $V_f = 2.778 \cdot 10^{-3}$ m/s; (1) $v_p = 0$; (2) $v_p = 0.02V_f$; (3) $v_p = 0.03V_f$; (4) $v_p = 0.05V_f$.

In Fig. 17a, the percentage of relative adsorptivity is plotted *versus* time for the lysozyme–anti-lysozyme system, when the interaction kinetics between the adsorbate and ligand do not occur infinitely fast (system in Fig. 7), and when the interaction kinetics

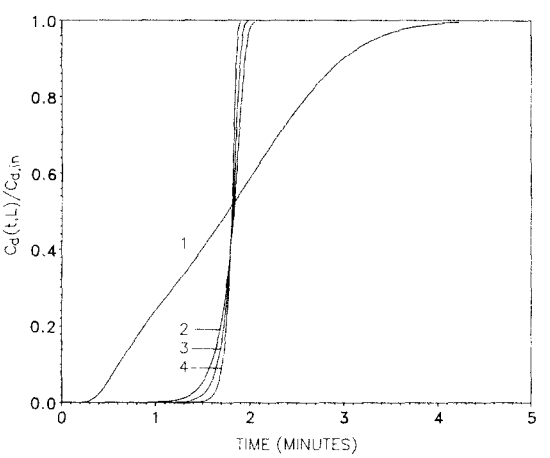

Fig. 16. Breakthrough curve of lysozyme when the dynamics of the interaction kinetics of the adsorption step are taken to be infinitely fast. $L = 0.03$ m; $z_0 = 16.120 \cdot 10^{-6}$ m; $V_f = 2.778 \cdot 10^{-3}$ m/s; (1) $v_p = 0$; (2) $v_p = 0.02V_f$; (3) $v_p = 0.03V_f$; (4) $v_p = 0.05V_f$.

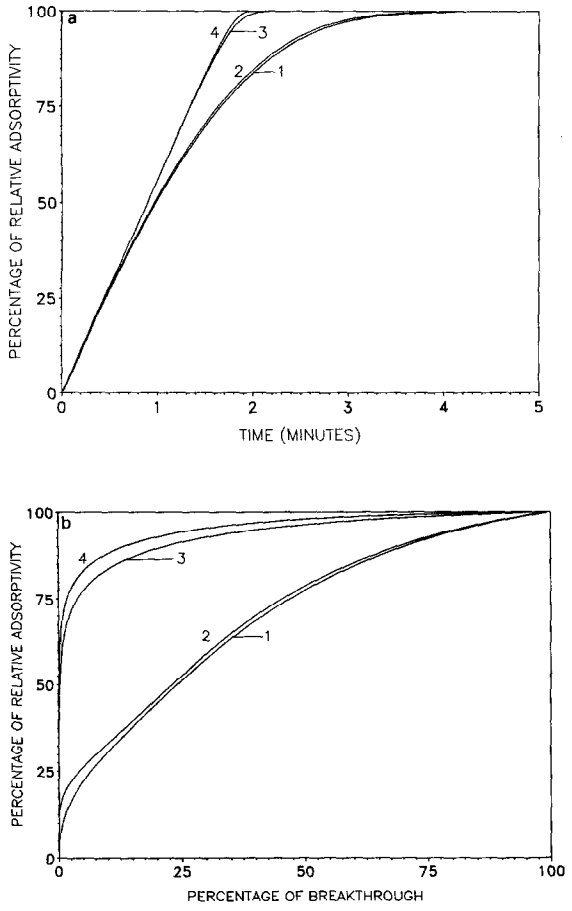

Fig. 17. Percentage of relative adsorptivity *versus* (a) time and (b) percentage of breakthrough for the lysozyme–monoclonal anti-lysozyme system when the dynamics of the interaction kinetics of the adsorption step are as follows: case I = finite (relatively fast) and case II = infinitely fast. $L = 0.03$ m; $z_0 = 16.120 \cdot 10^{-6}$ m; $V_f = 2.778 \cdot 10^{-3}$ m/s; (1) case I, $\nu_p = 0$; (2) case II, $\nu_p = 0$; (3) case I, $\nu_p = 0.02V_f$; (4) case II, $\nu_p = 0.02V_f$.

are taken to occur infinitely fast (system in Fig. 16); for the same adsorption system and conditions, the percentage of relative adsorptivity is plotted *versus* the percentage of breakthrough in Fig. 17b.

The results in Fig. 17a clearly show that, for a given time, the perfusive particles provide a higher percentage of relative adsorptivity than the percentage of relative adsorptivity obtained from the purely diffusive particles. However, for a given time and for the same value of ν_p, the data in Fig. 17a indicate that the differences in the values of the percentage of relative adsorptivity obtained from finite and infinitely fast interaction kinetics are small; it should be noted that the implications of the influence of ν_p and of the kinetics of interaction on column performance should be analyzed by considering simultaneously (by combining) the information obtained from Fig. 17a and b, as discussed earlier.

The results in Fig. 17b clearly show that, for a given percentage of breakthrough, the perfusive particles provide a higher percentage of relative adsorptivity than the percentage of relative adsorptivity obtained from the purely diffusive particles; however, the data in Fig. 17b indicate that for a given practical value of the percentage of breakthrough, the differences in the values of the percentage of relative adsorptivity obtained from finite and infinitely fast interaction kinetics are larger for the system involving perfusive particles. This latter result and the results obtained from the analysis of the data in Figs. 1–14 suggest that for adsorption systems having relatively fast or infinitely fast interaction kinetics, the use of perfusive particles could have the potential to provide improved column performance.

CONCLUSIONS

A mathematical model of perfusion chromatography has been constructed for column systems. The theoretical expression of the model could describe single- and multi-component adsorption in perfusive ($\nu_p > 0$) particles, and also in purely diffusive ($\nu_p = 0$) particles. The equations of the model for the adsorbent particles include the intraparticle mass transfer mechanisms of convection (intraparticle fluid flow) and diffusion, and the mass transfer step involving the interaction between the adsorbate molecules and the active sites on the surface of the porous adsorbent particles. The continuity expression for the fluid flowing stream in the column includes the mechanism of axial dispersion.

The perfusion chromatographic model was solved and used to study the dynamic behavior of column systems having perfusive or purely diffusive adsorbent particles of slab geometry. Two different adsorption systems were examined: one system considers the adsorption of β-galactosidase on immobilized monoclonal anti-β-galactosidase, and the other system involves the adsorption of lysozyme on

immobilized monoclonal anti-lysozyme. The values of the rate constants that characterize the dynamics of the interaction kinetics of the adsorption step are significantly different for these two adsorption systems. Whereas the dynamics of the interaction mechanisms for these two different adsorption systems are finite, a third case was also examined where the dynamics of the interaction mechanisms were considered to be infinitely fast. The dynamic behavior of column systems (frontal analysis studies) was examined for different column lengths (L), particle sizes (z_0), column fluid superficial velocities (V_f) and intraparticle fluid velocities (v_p), and for different values of the effective pore diffusivity (D_p) and of the parameter C_T that represents the highest concentration that the adsorbate could have in the adsorbed phase [the value of the parameter C_T could increase (decrease) if the total concentration of accessible active sites on the surface of the particles could increase (decrease)].

The results indicate that when the dynamics of the interaction kinetics of the adsorption step are relatively not fast and the column fluid superficial velocity is low, then the breakthrough curves obtained from column systems having perfusive particles are not significantly different from the breakthrough curves obtained from columns having purely diffusive particles; when the column fluid superficial velocity is high, then the breakthrough curves obtained from the columns involving perfusive particles are different from those obtained from columns with purely diffusive particles, and their differences become larger as the particle size increases.

When the dynamics of the interaction kinetics of the adsorption step are relatively fast or infinitely fast, the results show that the breakthrough curves obtained from column systems having perfusive particles are very steep, and the shape of the breakthrough curves was found (for the system conditions studied in this work) not to be significantly affected when the particle size (z_0) and the column fluid superficial velocity (V_f) were increased; on the contrary, the shape of the breakthrough curves obtained from column systems involving purely diffusive particles was found to be influenced significantly when the particle size and the column fluid superficial velocity were increased. Further, the steepness of the breakthrough curves obtained from columns having perfusive particles and the time at which breakthrough begins were found to increase with increasing intraparticle fluid velocity in the systems studied in this work. When the value of C_T of the perfusive particles was reduced by 10% relative to that of the purely diffusive particles, it was found that (for the systems examined here) the columns with the perfusive particles provided a higher percentage of relative adsorptivity than that obtained from the columns with the purely diffusive particles.

In conclusion, the results obtained from the systems studied in this work suggest that for adsorption systems having relatively fast or infinitely fast interaction kinetics (that is, the dynamics of the interaction step between the adsorbate molecules and the active sites are relatively fast or infinitely fast), the use of perfusive particles could have the potential to provide improved column performance.

ACKNOWLEDGEMENTS

The authors gratefully acknowledge support of this work by Monsanto and the NATO Scientific Affairs Division under Grant No. 880770.

SYMBOLS

A	molecule of adsorbate (expression 22)
AS	adsorbate–active site complex (expression 22)
C_d	concentration of adsorbate (single-component system) in the flowing fluid stream of the column, kg/m^3
C_{di}	concentration of component i (multi-component system) in the flowing fluid stream of the column, kg/m^3
$C_{d,in}$	concentration of adsorbate (single-component system) at $x < 0$ when $D_L \neq 0$, or at $x = 0$ when $D_L = 0$, kg/m^3
$C_{di,in}$	concentration of component i (multi-component system) at $x < 0$ when $D_{Li} \neq 0$, or at $x = 0$ when $D_{Li} = 0$, kg/m^3
C_p	concentration of adsorbate (single-component system) in pore fluid, kg/m^3
$\mathbf{C}_p$	vector of concentration variables defined after eqn. 9

C_{pi} concentration of component i (multi-component system) in pore fluid, kg/m^3
$\bar{C}_{psi}$ concentration variable defined in eqn. 16
C_s concentration of adsorbate (single-component system) in adsorbed phase, kg/m^3 particle
$\mathbf{C}_s$ vector of concentration variables defined after eqn. 9
C_{si} concentration of component i (multi-component system) in adsorbed phase, kg/m^3 particle
C_T maximum equilibrium concentration of adsorbate (single-component system) in adsorbed phase when all accessible active sites are utilized (eqn. 24), kg/m^3 particle
D_L axial dispersion coefficient of adsorbate (single-component system), m^2/s
D_{Li} axial dispersion coefficient of component i (multi-component system), m^2/s
D_p effective pore diffusion coefficient of adsorbate (single-component system), m^2/s
$\mathbf{D}_p$ effective pore diffusivity matrix (multi-component system)
D_{pij} effective pore diffusion coefficients of multi-component system (terms of the effective pore diffusivity matrix), m^2/s
$\mathbf{D}_s$ surface diffusivity matrix (multi-component system)
D_s surface diffusion coefficient of adsorbate (single-component system), m^2/s
D_{sij} surface diffusion coefficients of multi-component system (terms of the surface diffusivity matrix), m^2/s
dV volume differential in eqns. 16 and 19
$f_i(\mathbf{C}_p, \mathbf{C}_s, \mathbf{k})$ functional form defined after eqn. 9
$g_i(\mathbf{C}_p, \mathbf{K})$ functional form defined after eqn. 11
K equilibrium adsorption constant of adsorbate (single-component system), $K = k_1/k_2$, m^3/kg
$\mathbf{K}$ vector of equilibrium adsorption constants defined after eqn. 11
$\mathbf{k}$ vector of adsorption rate constants defined after eqn. 9
K_p permeability of the porous adsorbent particle (eqn. 20), m^2
k_1 adsorption rate constant in eqn. 23, m^3/kg · s
k_2 adsorption rate constant in eqn. 23, s^{-1}
l total number of components adsorbed by specific and non-specific adsorption (multi-component system)
L column length, m
n total number of components in multi-component system
r radial distance in adsorbent particle of spherical geometry, m
r_0 radius of spherical adsorbent particle, m
S active site (expression 22)
T temperature, K
t time, s
V_f column fluid superficial velocity, m/s
v_p intraparticle fluid velocity (intraparticle convective velocity), m/s
V_{pv} volume of adsorbent particle, m^3
x axial distance, m
z space coordinate of adsorbent particle of slab geometry, m
z_0 length (size) of adsorbent particle of slab geometry, m

Greek letters

α_1 constant in eqn. 20
α_2 constant in eqn. 20
ε void fraction in column
ε_p void fraction in porous adsorbent particle

REFERENCES

1 N. B. Afeyan, N. F. Gordon, I. Mazsaroff, L. Varady, S. P. Fulton, Y. B. Yang and F. E. Regnier, *J. Chromatogr.*, 519 (1990) 1.
2 J. H. Petropoulos, J. K. Petrou and A. I. Liapis, *Ind. Eng. Chem. Res.*, 30 (1991) 1281.
3 J. H. Petropoulos, A. I. Liapis, N. P. Kolliopoulos, J. K. Petrou and N. K. Kanellopoulos, *Bioseparation*, 1 (1990) 69.
4 A. I. Liapis and D. W. T. Rippin, *Chem. Eng. Sci.*, 32 (1977) 619.
5 A. I. Liapis and D. W. T. Rippin, *Chem. Eng. Sci.*, 33 (1978) 593.
6 M. Balzli, A. I. Liapis, and D. W. T. Rippin, *Trans. Inst. Chem. Eng.*, 56 (1978) 145.
7 A. I. Liapis and D. W. T. Rippin, *AIChE J.*, 25 (1979) 455.
8 A. I. Liapis and R. J. Litchfield, *Chem. Eng. Sci.*, 35 (1980) 2366.
9 D. M. Ruthven, *Principles of Adsorption and Adsorption Processes*, Wiley, New York, 1984.
10 B. H. Arve and A. I. Liapis, *AIChE J.*, 33 (1987) 179.
11 D. M. Ruthven, in A. I. Liapis (Editor), *Fundamentals of Adsorption*, Engineering Foundation, New York, 1987, pp. 29–49.

12 B. H. Arve and A. I. Liapis, *Biotechnol. Bioeng.*, 32 (1988) 616.
13 A. I. Liapis, *J. Biotechnol.*, 11 (1989) 143.
14 P. C. Wankat, *Rate-Controlled Separations*, Elsevier Applied Science Publ., Barking, 1990.
15 A. I. Liapis, *Sep. Purif. Methods*, 19 (1990) 133.
16 M. A. McCoy and A. I. Liapis, *J. Chromatogr.*, 548 (1991) 25.
17 F. H. Arnold, H. W. Blanch and C. R. Wilke, *Chem. Eng. J.*, 30 (1985) B9.
18 J. H. Harwell, A. I. Liapis, R. J. Litchfield and D. T. Hanson, *Chem. Eng. Sci.*, 35 (1980) 2287.
19 C. J. Geankoplis, *Transport Processes and Unit Operations*, Allyn & Bacon, Boston, 2nd ed., 1983.
20 F. H. Arnold, H. W. Blanch and C. R. Wilke, *Chem. Eng. J.*, 30 (1985) B25.
21 W. Norde, *Adv. Colloid Interface Sci.*, 25 (1986) 267.
22 A. I. Liapis, in A. B. Mersmann and S. E. Scholl (Editors), *Fundamentals of Adsorption*, Engineering Foundation, New York, 1990, pp. 25–61.
23 A. I. Liapis, A. B. Anspach, M. E. Findley, J. Davies, M. T. W. Hearn and K. K. Unger, *Biotechnol. Bioeng.*, 34 (1989) 467.
24 H. L. Toor and K. R. Arnold, *Ind. Eng. Chem., Fundam.*, 4 (1965) 363.
25 A. I. Liapis and R. J. Litchfield, *Trans. Inst. Chem. Eng.*, 59 (1981) 122.
26 I. Lundstrom, B. Ivarsson, U. Jonsson and H. Elwing, in W. J. Feast and H. S. Munro (Editors), *Polymer Surfaces and Interfaces*, Wiley, New York, 1987, pp. 201–230.
27 R. L. Beissinger and E. F. Leonard, *J. Colloid Interface Sci.*, 85 (1982) 521.
28 A. L. Myers, in A. I. Liapis (Editor), *Fundamentals of Adsorption*, Engineering Foundation, New York, 1987, pp. 3–25.
29 E. C. Moreno, M. Kresak, J. J. Kane and D. I. Hay, *Langmuir*, 3 (1987) 511.
30 D. P. Valenzuela and A. L. Meyers, *Adsorption Equilibrium Data Handbook*, Prentice Hall, Englewood Cliffs, NJ, 1989.
31 O. Talu and I. Zweibel, *AIChE J.*, 32 (1986) 1263.
32 C. M. Shu, S. Kulvaranon, M. E. Findley and A. I. Liapis, *Sep. Technol.*, 1 (1990) 18.
33 B. H. Arve, *Ph.D. Dissertation*, Department of Chemical Engineering, University of Missouri–Rolla, Rolla, MO, 1986.
34 M. A. McCoy, *Report Number 5*, Department of Chemical Engineering, University of Missouri-Rolla, Rolla, MO, 1991.
35 R. B. Bird, W. E. Stewart and E. N. Lightfoot, *Transport Phenomena*, Wiley, New York, 1960.
36 J. Villadsen and M. L. Michelsen, *Solution of Differential Equation Models by Polynomial Approximation*, Prentice-Hall, Englewood Cliffs, NJ, 1978.
37 C. D. Holland and A. I. Liapis, *Computer Methods for Solving Dynamic Separation Problems*, McGraw-Hill, New York, 1983.
38 T. Wicks, *Scientific Computing and Analysis Library Report*, SCA-LR-52, Boeing Computer Services, Seattle, WA, 1988.
39 M. A. McCoy, B. J. Hearn and A. I. Liapis, *Chem. Eng. Commun.*, 108 (1991) 225.